

# Dental Depth Profilometric Diagnosis of Pit & Fissure Caries Using Frequency-Domain Infrared Photothermal Radiometry and Modulated Laser Luminescence

---

Raymond J. Jeon, Calvin Han, Andreas Mandelis\* and Victor Sanchez

Center for Advanced Diffusion-Wave Technologies Department of Mechanical and Industrial Engineering, University of Toronto, 5 King's College Road, Toronto, Ontario, M5S 3G8, Canada

Stephen H. Abrams

Four Cell Consulting, 748 Briar Hill Avenue, Toronto, Ontario, M6B 1L3, Canada

## Abstract

Non-intrusive, non-contacting frequency-domain photothermal radiometry (FD-PTR or PTR) and frequency-domain luminescence (FD-LUM or LUM) have been used with a 659-nm laser source to assess the pits and fissures on the occlusal surfaces of human teeth. Fifty-two human teeth were examined with simultaneous measurements of PTR and LUM and compared to conventional diagnostic methods including continuous (dc) luminescence (DIAGNOdent), visual inspection, and radiographs. To compare each method, sensitivities and specificities were calculated by using histological observations as the gold standard. With the combined criteria of 4 PTR and LUM signals (2 amplitudes and 2 phases), it was found that the sensitivity of this method was much higher than any of the other methods used in this study; whereas, the specificity was comparable to that of dc luminescence diagnostics. Therefore, PTR and LUM, as a combined technique, has the potential to be a reliable tool to diagnose early pit and fissure caries and could provide detailed information about deep lesions with its depth profilometric character.

## Introduction

Over the last few decades, with the widespread use of fluoride, the prevalence of caries, particularly smooth surface caries, has been considerably reduced [McComb and Tam, 2001; Ricketts et al., 1997]. This reduction in smooth surface caries has resulted in an increase in the proportion of small lesions in the pits and fissures of teeth [McComb and Tam, 2001]. The diagnosis of pit and fissure caries continues to be a dilemma for clinicians. Caries detection for the vast majority of clinicians still relies upon radiographs, explorer, and visual determination. With these “crude” tools, clinicians are hampered in their ability to diagnose and monitor the carious lesion or assess the status of a stained pit or fissure. There are no clear guidelines on their clinical management, and one clinical research group has suggested that carious defects are almost always present under stained pits and fissures of non-smokers [CRA Newsletter, 1999]. The development of a non-invasive, non-contacting technique or instrument, which can detect early demineralization on or beneath the enamel surface, is essential for the clinical management of this problem.

The use of lasers for dental diagnostics is considered to be promising, mainly through the phenomenon of laser-induced fluorescence of the enamel. Eggertsson et al. [1999] evaluated the uses of laser fluorescence (LF) and dye-enhanced laser fluorescence (DELFL), compared them to visual examination, and found DELFL was better in sensitivity, but DELFL and visual examination were better than LF in specificity. In an effort to quantify the fluorescence-based light-induced fluorescence (QLF) technique, various devices such as a ring illuminator, a beam splitter, and a clinical caries camera were compared by Lagerweij et al. [1999]. DIAGNOdent [Hibst and Konig, 1994; Hibst et al., 2000] uses continuous (dc) laser excitation to distinguish between carious and healthy tooth structure. The device is based upon the fluorescence caused by porphyrins present in carious tissue and not the amount of enamel demineralization [Alwas-Danowska et al., 2002]. Porphyrin fluorescence may lead to false positives since these are also found in stained, healthy fissures [Hibst and Paulus, 1999; Welsh et al., 2000]. A number of studies were performed to assess the feasibility of using this device [Lussi et al., 1999; Shi et al., 2001; Shi et al., 2000], and it has been evaluated as having the potential to improve caries assessment in many ways. Specifically, its high reproducibility was claimed to be an outstanding benefit of this device. Nevertheless, a validity study involv-

ing the DIAGNOdent concluded that using dc luminescence was not statistically significantly different from visual inspection [Alwas-Danowska et al., 2002]. Furthermore, it was concluded that DIAGNOdent was suitable for detecting small superficial lesions, rather than deep dentinal lesions [Alwas-Danowska et al., 2002]. There are various sensitivity and specificity values obtained for DIAGNOdent, and they differ widely among different researchers, 0.76 ~ 1.00 for the sensitivity and 0.47 ~ 0.94 for the specificity [Lussi et al., 1999; Lussi et al., 2001; Heinrich-Weltzien et al., 2002; Costa et al., 2002; Alwas-Danowska et al., 2002; Anttonen et al., 2003].

The first attempt to apply the depth profilometric capability of frequency-domain laser infrared photothermal radiometry (PTR) toward the inspection of dental defects was reported by Mandelis et al. [2000] and Nicolaidis et al. [2000] and was recently reviewed by Mandelis [2002]. The approach of these investigators consists of a combined dynamic (i.e., non-static, steady-state signal level) dental depth profilometric inspection technique, which can provide simultaneous measurements of intensity-modulated frequency-domain PTR (FD-PTR), and luminescence (FD-LUM) signals from defects in teeth. FD-PTR is an evolving technology and has been applied, among other areas, to the non-destructive evaluation (NDE) of sub-surface features in opaque materials [Busse and Walther, 1992]. It has shown promise in the study of excited-state dynamics in optically active, solid-state (laser) materials [Mandelis et al., 1993]. The technique is based on the modulated thermal infrared (black-body or Planck radiation) response of a medium, resulting from radiation absorption and non-radiative energy conversion followed by temperature rise (in the case of dental interrogation, less than 1°C). The generated signals carry sub-surface information in the form of a temperature depth integral. Thus, PTR has the ability to penetrate and yield information about an opaque medium well beyond the range of optical imaging. Specifically, the frequency dependence of the penetration depth of thermal waves makes it possible to perform depth profiling of materials [Munidasa and Mandelis, 1992]. In PTR applications to turbid media, such as hard dental tissue, depth information is obtained following optical-to-thermal energy conversion of the incident laser power in two distinct modes: conductively, from a near-surface distance controlled by the thermal diffusivity of enamel (50 ~ 500 µm); and radiatively, through blackbody emissions from considerably deeper regions commensurate with the optical penetration of the

diffusely scattered laser-induced optical field (several mm) [Nicolaidis et al., 2002].

It is often desirable in dental practice to obtain detailed information on potential lesions or to examine pits and fissures with high spatial resolution, using a focused laser source. To meet these objectives, recently, a combination of FD-PTR and FD-LUM was used as a fast dental diagnostic tool to quantify sound enamel or dentin as well as sub-surface cracks in human teeth [Nicolaidis et al., 2000]. Under 488-nm laser excitation and frequencies in the range of 10 Hz ~ 10 kHz, it was found that PTR images are complementary to LUM images as a direct result of the complementary nature of non-radiative and radiative de-excitation processes, which are responsible for the PTR and LUM signal generation, respectively, at that wavelength. It was also concluded qualitatively that radiometric images are depth profilometric (meaning they yield depth-dependent information as a function of the laser-beam modulation frequency), but no definitive conclusions regarding the depth profilometric character of LUM were reached. Finally, LUM frequency responses from enamel and hydroxyapatite were found to exhibit two relaxation lifetimes, the longer of which ( $\sim ms$ ) is a benchmark hydroxyapatite relaxation lifetime common to all teeth and is not sensitive to the defect state or the overall quality of the enamel. A degree of sensitivity to enamel quality was established for the shorter ( $\sim \mu s$ ) lifetime. Our group has introduced theoretical models of FD-PTR and FD-LUM which can yield quantitative values of optical and fluorophore parameters of sound enamel [Nicolaidis et al., 2002]. Unique sets of the optical parameters ( $\mu_a$ : optical absorption coefficient,  $\mu_s$ : scattering coefficient,  $\mu_{IR}$ : spectrally averaged infrared emission coefficient) of enamel and its fluorophore relaxation time constants ( $\tau_1$ ,  $\tau_2$ ) were obtained using the combined diffuse photon-density-wave and thermal-wave theory with a three-dimensional photothermal multi-parameter fit formulation and inputs from LUM and PTR data [Nicolaidis et al., 2002]. More recently, it was found that PTR (alone or in combination with LUM) could be used as a sensitive, depth-profilometric dental probe for the diagnosis of near-surface or deep sub-surface carious lesions and/or for monitoring enamel thickness [Jeon et al., 2003].

In this study, 52 human teeth were examined to evaluate the diagnostic capabilities of FD-PTR and FD-LUM and compared to DIAGNOdent as well as visual inspection and radiographs. After the measurements were completed,

the teeth were sectioned. Histological findings were used as the gold standard to calculate and compare the sensitivity and the specificity of all the diagnostic methodologies used in this study.

## **Materials and Methods**

Fifty-two extracted human teeth (25 molars, 21 bicuspid and 6 primary molars) were evaluated. The measured points included, at a minimum 2 healthy areas and 2 fissures on the occlusal surface and 1 healthy point on the smooth side surface. A few more measured points were added for each tooth, so the total measurement sample finally consisted of 332 points, including 104 healthy points, 176 fissures on the occlusal surface, and 52 healthy points on the smooth surfaces of the teeth. In order to compare our experimental results to other clinical methods, 5 dentists examined and ranked the set of teeth by visual inspection and radiographs. DIAGNOdent (KAVO type 2095) measurements were also obtained from the occlusal surfaces of the teeth.

Teeth samples were stored in saline solution (0.9% Sodium Chloride) separately in vials before the experiments to avoid dehydration and contamination. The occlusal surface of each tooth was photographed with a CCD camera (PULNiX TMC-73M) with a magnification lens (NAVITAR Zoom6000) and the measurement points were selected and marked on each photograph.

### ***Visual Inspection***

Five clinicians were given sample teeth which had been stored in saline and asked to assess the teeth with respect to clinical criteria. They were asked to only assess the occlusal surface of the tooth, specifically, the pits and fissures. The clinicians were not asked to state whether the caries was in enamel or dentin but whether they would treat the tooth and in what manner. This is very similar to what one does clinically on a day-to-day basis. We provided each clinician with a tooth, explorer, oil free air, and a radiograph of the tooth. The clinicians were asked to assign a ranking from 1 to 10 for each tooth with 1 meaning no treatment was required and 10 meaning that a large carious lesion was present involving the dentin and enamel (see table 1). The clinicians were not asked to assess each fissure, only to rank the status of all fissures on the occlusal

General Description of Levels of Caries [Lussi et al., 1999]	Visual Inspection (1~10)	DIAGNOdent (0~99) [Lussi et al., 1999]	Radiograph	Histological Observation
D <sub>0</sub> : Intact			Healthy: Indicating no sign of demineralization	Sound enamel or Healthy fissure
D <sub>1</sub> : no caries, or histological enamel caries limited to the outer half of the enamel thickness	1 ~ 2 Incipient or Healthy	0-4	Enamel caries under 1/2 the distance to DEJ	Demineralized fissure but solid enamel base; very good enamel thickness to the pulp; at least 1/2 thickness of enamel remains intact
D <sub>2</sub> : histological caries extending beyond the outer half, but confined to the enamel	3 ~ 5 Fissure Sealant	4.01 ~ 10	Enamel caries greater than 1/2 the distance to DEJ	Demineralizes fissure but solid enamel base
D <sub>3</sub> : histological dentinal caries limited to the outer half of the dentin thickness	6 ~ 8 Restore the Fissure	10.01 ~ 18		
D <sub>4</sub> : histological dentinal caries extending into the inner half of dentin thickness	9 ~ 10 Deep Dentin Caries	> 18.01	Dentin caries	Caries into dentin

TABLE 1. Diagnostic criteria for the Visual Inspection, DIAGNOdent, X-ray and Histological Observation.

surface. Rankings were further divided into four groups with the classifications as shown in table 1.

***Radiographic Examination***

A radiograph was taken on each tooth using standard dental x-rays. The teeth were each mounted on a jig that fixed the distance between film, tooth, and x-ray tube head. This ensured similar magnification and exposure. Each radiograph was examined by two clinicians independently to detect the presence of occlusal caries.

***DIAGNOdent***

Each tooth was dried and a DIAGNOdent instrument (KAVO type 2095) was used to obtain readings from the occlusal surface. The machine was calibrated between each tooth and the surface was scanned 3 times to confirm the reading. The highest reading and its location was recorded. The readings were

assessed and ranked using the criteria developed by Lussi et al. [1999] and listed in table 1.

### ***Sample Preparation Before PTR and LUM Scanning***

Each sample tooth in the study was removed from the vial and was rinsed thoroughly with clean water for more than 20 seconds and then was dried with pressurized air. Then, the tooth was placed on the sample stage, and the laser was turned on and focused on the sample tooth by adjusting a 3-axis micrometer stage. This process usually took about 20 minutes before starting measurements, during which time the tooth was dehydrated properly. This protocol was adhered to, because dehydration of a tooth sample affects its optical qualities, such as light scattering and fluorescence as well as thermal properties. al-Khateeb et al. [2002] showed that the fluorescence radiance of sound enamel and enamel lesions decreased from that of the wet enamel for about 2 to 20 minutes, depending on the sample, before becoming steady. Therefore, 20 minutes of preparation time appears to be necessary to avoid the effects of dehydration or the signals. Moreover, since the surface temperature of the sample could be slightly decreased during washing it with water and drying it with compressed air, there is need to wait until the sample temperature reaches its ambient value, because modulated luminescence and thermal infrared (blackbody) emissions may be affected by the background temperature.

### ***PTR and LUM Measurements***

Figure 1 shows the experimental setup for combined frequency-domain PTR and LUM probing. A semiconductor laser with a wavelength of 659 nm and maximum power of 30 mW (Mitsubishi ML1016R-01) was used as the source of both PTR and LUM signals. A diode laser driver (Coherent 6060) was triggered by the built-in function generator of the lock-in amplifier (Stanford Research SR830), modulating the laser current harmonically. The laser beam was focused on the sample with a high performance lens (Gradium GPX085) to a spot size of approximately 55  $\mu\text{m}$ . The modulated infrared PTR signal from the tooth was collected and focused by two off-axis paraboloidal mirrors onto a Mercury Cadmium Telluride (HgCdTe or MCT) detector (EG&G Judson J15D12-M204-S050U). Before being sent to the lock-in amplifier, the PTR signal was amplified by a preamplifier (EG&G Judson PA-300). For the simultaneous measurement of PTR and LUM signals, a germanium window was placed

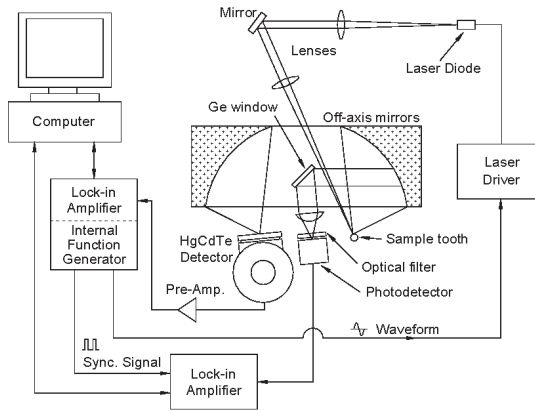


FIG. 1: Schematic diagram of experimental setup.

between the paraboloidal mirrors so that wavelengths up to  $1.85 \mu\text{m}$  (Ge bandgap) would be reflected and absorbed, while infrared radiation with longer wavelengths would be transmitted. The reflected luminescence was focused onto a photodetector of spectral bandwidth  $300 \text{ nm} \sim 1.1 \text{ mm}$  (Newport 818-BB-20). A cut-on colored glass filter (Oriel 51345, cut-on wavelength:  $715 \text{ nm}$ ) was placed in front of the photodetector to block laser light reflected or scattered by the tooth. For monitoring the modulated luminescence, another lock-in amplifier (EG&G model 5210) was used. Both lock-in amplifiers were connected to, and controlled by, the computer via RS-232 ports.

This experimental set-up needed a wide angle ( $\sim 80^\circ$ ) between laser beam and detector to detect infrared signals coming from the tooth surface. This restriction created problems detecting signals from fissures with a narrow entrance angle, or fissures that tracked under a cuspal incline (especially mandibular premolars), or headed off on an extreme angle with respect to the occlusal surface. At each measurement point, a frequency scan was performed measuring the PTR and the LUM signals by varying the frequency from  $1 \text{ Hz}$  to  $1 \text{ kHz}$ . Frequency range has been segmented into 40 equal intervals in a logarithmic scale by a data acquisition computer program and the frequency was incremented to the next value after each measurement. There was a 15-second time delay between the measurements at each frequency to allow for thermalization of the tooth surface, which was necessary for stabilizing the signals.

### *Histology Observation*

After all the measurements were finished, the teeth in our sample were sectioned and photographed with the CCD camera perpendicular to the surface at each measurement point. The photographs of the sectioned teeth were examined and ranked according to the criteria listed in table 1.

### *Statistical Analysis Methodology*

In order to assess PTR and LUM as caries diagnostic techniques and compare them (combined and separately) to the other conventional probes, sensitivities and specificities were calculated at two different thresholds ( $D_2$ ) and ( $D_3$ ) as defined in table 1 for all the diagnostic methods. While the PTR and LUM signals were taken from all 280 occlusal measurement points, only 1 or 2 points on each tooth were assessed by the other examination methods. Therefore, each calculation only used the corresponding measurement points. To create suitable criteria for assessing the carious state via PTR and LUM, the general characteristics of the respective signals and their converting equations, listed in table 2, were used. Those characteristics were established from the experimental results of the frequency scans with carious and healthy tooth samples. In the case of the PTR amplitude as shown in figure 2(e), the shape of the

Signal	General characteristics	Converting equation to determine numeric ranking
PTR amplitude	<ul style="list-style-type: none"> <li>The shape for a healthy spot in log-log plot is almost linear from low frequency (1 Hz) to high frequency (1000 Hz).</li> <li>Unhealthy (demineralized surface, enamel caries or dentin caries) spots show greater amplitude at all frequency range compared to healthy spots.</li> <li>Unhealthy spot shows a curvature (greater than the linear line) in the frequency range of 10 ~ 100 Hz in logarithm plot.</li> </ul>	<ul style="list-style-type: none"> <li>(slope at low frequency) — (slope at high frequency)</li> <li>average at 4 frequencies</li> </ul>
PTR phase	<ul style="list-style-type: none"> <li>The shape for the healthy spot in log (freq.) - linear (phase) plot is almost linear from low frequency (1 Hz) to high frequency (1000 Hz).</li> <li>Unhealthy spots show higher phase at low frequency range and inverse at high frequency range than healthy spots.</li> </ul>	<ul style="list-style-type: none"> <li>(average of phases at 2 low frequencies (1,6.68 Hz)) – (average of phases at 2 high frequencies (211.35, 1000 Hz))</li> </ul>
LUM amplitude	<ul style="list-style-type: none"> <li>Both healthy and unhealthy spot show same shape: higher amplitude at low frequency range than at high frequency range.</li> <li>Unhealthy spots show greater amplitude than healthy ones.</li> </ul>	<ul style="list-style-type: none"> <li>average at 3 frequencies (1, 211.35, 501.18 Hz)</li> </ul>
LUM phase	<ul style="list-style-type: none"> <li>At only high frequency range (&gt; 100 Hz), unhealthy spots show greater phase than healthy ones.</li> </ul>	<ul style="list-style-type: none"> <li>one phase signal at high frequency (501.18 Hz)</li> </ul>

TABLE 2. Characteristics of frequency scan curves of PTR and LUM.

frequency scan curve for the healthy spot on a log-log plot is almost linear from low frequency (1 Hz) to high frequency (1000 Hz), while unhealthy spots (demineralized surface, enamel caries, or dentin caries) exhibit larger amplitude than healthy spots over the entire frequency range and a pronounced curvature with a “knee” at certain frequency ranges on the logarithmic plot as shown in figure 3(c). The PTR phase shape for the healthy spot on a linear (phase)—log (frequency) plot, as shown in figure 2(f), is almost linear across all frequencies (1 Hz ~ 1 kHz), while unhealthy spots in figure 3(d) exhibit larger phases at low frequencies and cross the healthy phase range at intermediate frequencies. There is no difference in the LUM amplitude shape between healthy and unhealthy spots as shown in figures 2(g) and 3(e). The shape of the amplitude curves is consistent throughout, decreasing from low to high frequencies. The LUM amplitude curves for unhealthy spots in figure 3(e) lie above the healthy band over the entire frequency range. The LUM phase shows slight differences between healthy points, figure 2(h), and carious points, figure 3(f). In general, carious regions exhibit larger LUM phase lags than healthy spots but only at the high frequency end ( $> 100$  Hz); figures 2(h) and 3(f).

We established the mean values for PTR amplitude and phase, and LUM amplitude and phase from all the healthy, smooth surface points on the tooth samples. This allowed us to examine the behavior of healthy tooth structure without the influence of fissure geometry or the effects of varying enamel thickness in the fissure. A series of mean values and standard deviations vs. frequency curves were developed for each signal and plotted for each tooth. This allowed us to compare the behavior of each probed point to a healthy smooth surface area.

## Experimental Results

### *PTR and LUM Measurements*

Typical healthy and carious tooth samples and their PTR and LUM frequency responses are shown in figures 2 and 3, respectively. To identify each probed point, upper case letters and serial numbers were assigned: F for fissure, HI for healthy inclined occlusal surface, and HS for healthy smooth surfaces. Also, the mean values from all healthy smooth surface points at each frequency and their standard deviation bars were added to each plot to compare the various curves.

Fig. 2

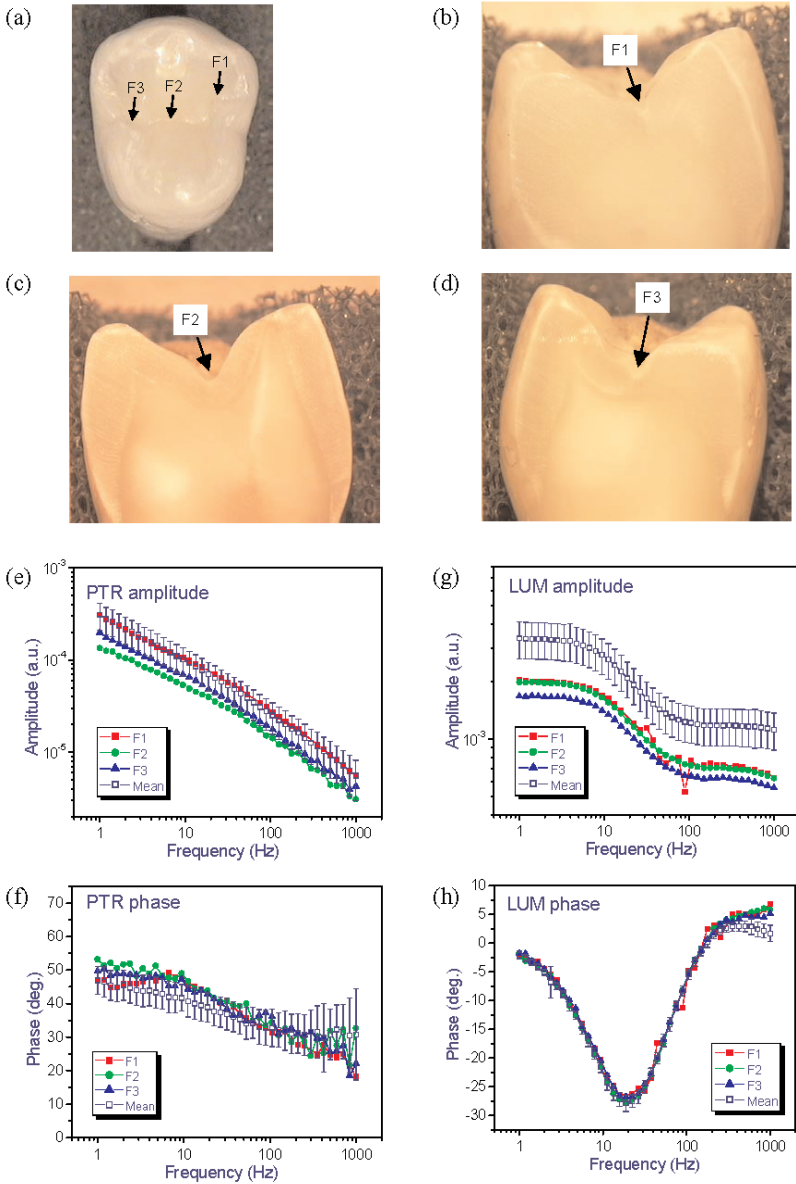


FIG. 2: A healthy tooth sample and its PTR and LUM signals. (a) occlusal view of the tooth; (b-d) cross-sectioned view of each measuring point, F1, F2 and F3; (e,f) PTR and (g,h) LUM amplitude and phase frequency scans at all the measuring points with the healthy mean value and population-weighted standard deviation.

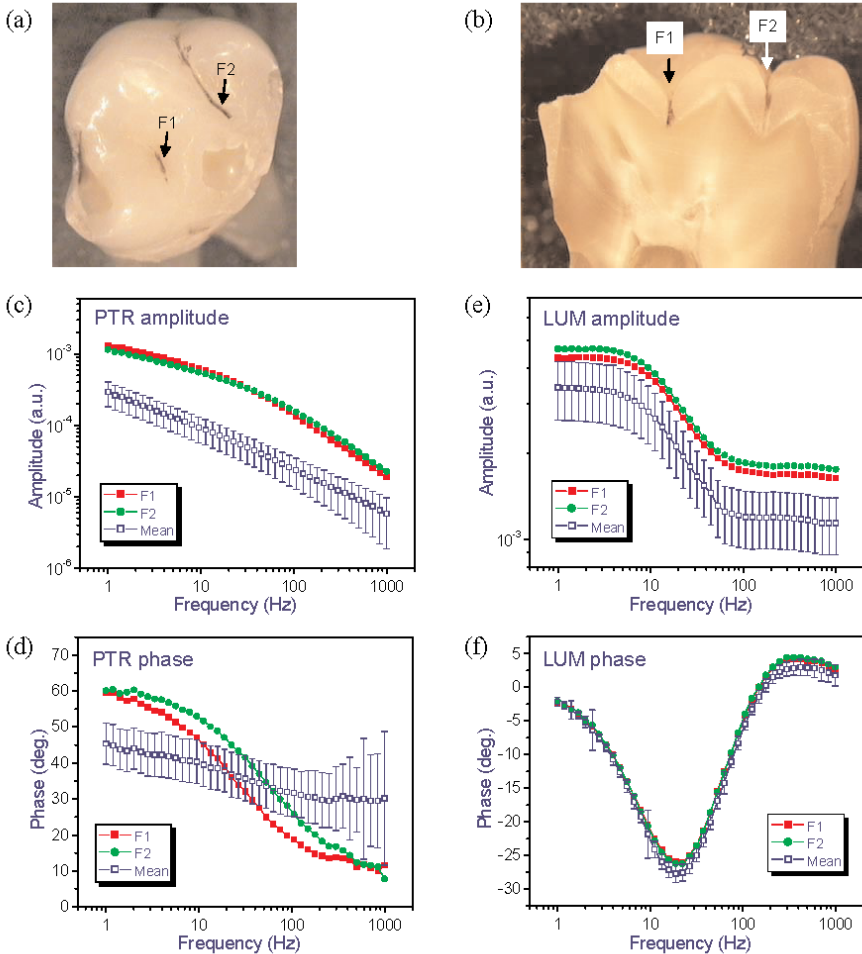


FIG. 3: A carious tooth sample and its PTR and LUM signals. (a) occlusal view of the tooth; (b) cross-sectioned view of each measuring point, F1 and F2; (c,d) PTR and (e,f) LUM amplitude and phase frequency scans at all the measuring points with the healthy mean value and population-weighted standard deviation.

### Healthy Occlusal Fissures

Figure 2(a) shows the occlusal surface of a healthy tooth and its associated measured points. This tooth had a DIAGNOdent reading of 4 and average visual inspection ranking of 1.4 and no evidence on the radiographs of any caries. These results indicated that there was no evidence of pathology in the fissures of this

tooth. Histological observation shown in figures 2(b)—2(d) also verified that all the measured points were healthy. In figure 2(e), all PTR amplitude curves are located in-between the standard deviation band or lower than the lower bound of standard deviation, which is believed to be a healthy spot as long as other signals do not show unhealthy behavior and have a curve shape consistent with the healthy mean-value curve. PTR phase curves for fissures in figure 2(f) are slightly higher than the healthy mean. In general, a healthy tooth exhibits weaker PTR signals than carious teeth. This is the cause of poorer signal-to-noise ratios (SNR) in both amplitude and phase curves. LUM amplitude curves for all probed points are below the healthy band in figure 2(g). LUM amplitudes and phases suffer from low SNR in the high frequency range.

### *Carious Occlusal Fissures*

The carious tooth in figure 3 had a DIAGNOdent reading of 12 in the mesial pit and a clinical ranking of 3.80. The radiograph did not indicate the presence of any carious lesion on the occlusal surface. There was a carious lesion on the distal surface of this tooth but this was not the area under examination. This carious tooth exhibits clear differences from the healthy mean curves, as shown in figures 3(c-f). PTR amplitude curves for the fissures in figure 3(c) show larger amplitude at all frequencies and a curvature in the mid-frequency range. PTR phases for the carious fissure in figure 3(d) also show non-healthy features: a larger phase lag at low frequencies and a steep slope resulting in a cross-over with the healthy band at intermediate frequencies. LUM amplitude and phase ( $f > 100$  Hz) for the carious spots in figures 3(e,f) are also higher than the healthy band.

### *Carious Fissure Revealed Only with PTR and LUM*

In figure 4, this mandibular second premolar illustrates the accuracy of PTR and LUM. The tooth had a DIAGNOdent reading of maximum 10 and average visual inspection ranking of 2.2, indicating that a clinician would need to watch or monitor the fissures. There was no indication on the radiographs of any caries being present. Nevertheless, PTR and LUM signals, including all information from the amplitude and phase responses over the entire frequency scan (1 Hz ~ 1 kHz), indicate that F2 and F3 have caries into dentin. Histological observation results show that this is, indeed, the case for these two points, as well as for point F1. The signals from fissure F1 show the influence that fissure geometry, angle of the mouth of the fissure, or the direc-

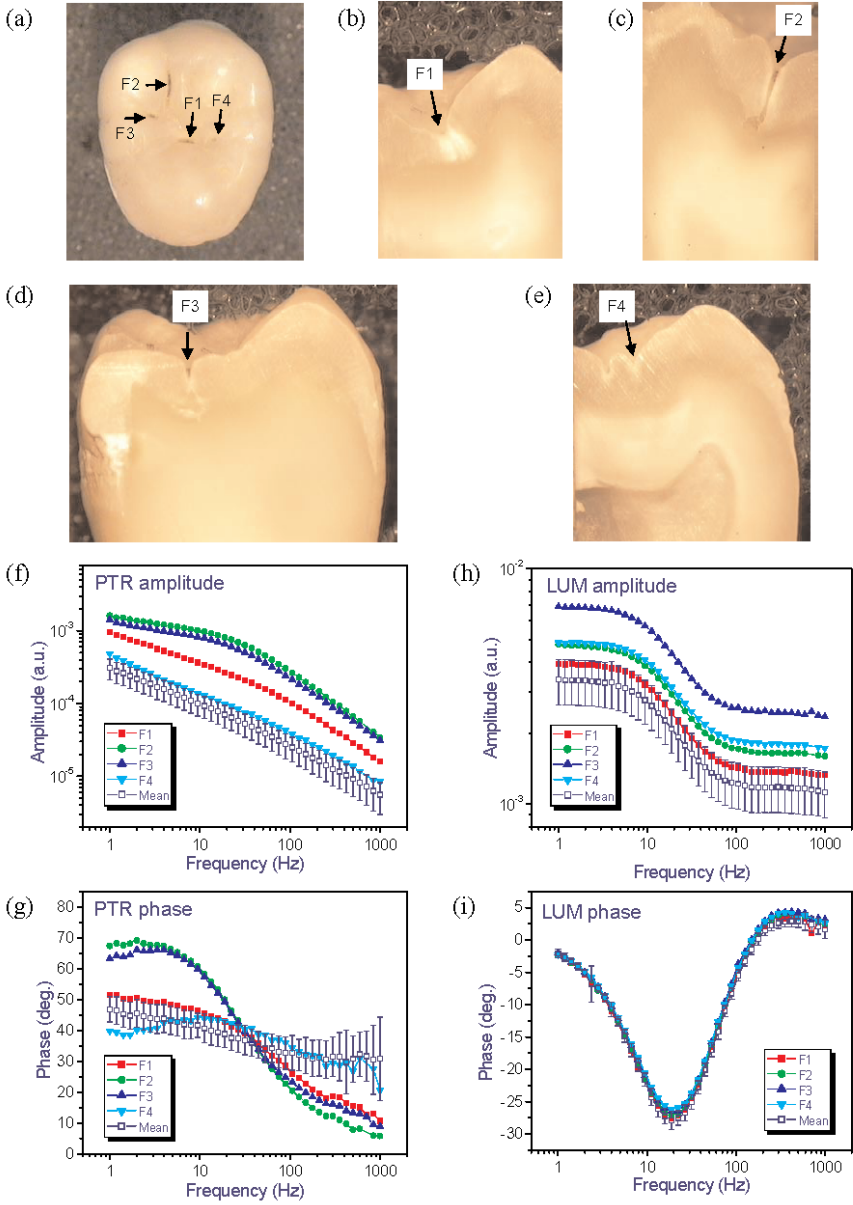


FIG. 4: Another tooth sample and its PTR and LUM signals. (a) occlusal view of the tooth; (b-e) cross-sectioned view of each measuring point, F1, F2, F3 and F4; (f,g) PTR and (h,i) LUM amplitude and phase frequency scans at all the measuring points with the healthy mean value and population-weighted standard deviation.

Examination method	Sensitivity threshold (D <sub>2</sub> /D <sub>3</sub> )	Specificity threshold (D <sub>2</sub> /D <sub>3</sub> )	Size of sample (# of points)
PTR and LUM combined	0.81 / 0.79	0.87 / 0.72	280
PTR only	0.69 / 0.52	0.86 / 0.72	280
LUM only	0.61 / 0.58	0.81 / 0.77	280
Visual Inspection	0.51 / 0.36	1.00 / 1.00	52
Radiograph	0.29 / 0.36	1.00 / 0.85	52
DIAGNOdent	0.60 / 0.76	0.78 / 0.85	131

TABLE 3. Sensitivities and specificities at the caries level of enamel (D<sub>2</sub>) and the caries level of dentin (D<sub>3</sub>) for various examination methods.

tion of the fissure base may have in the generation of PTR and LUM signals. The PTR amplitude of F1 in figure 4(f) is above the healthy band and the PTR phase in figure 4(g) also shows clear departure from the healthy band in the high frequency range. PTR and LUM curves of the healthy fissure F4 are located within the healthy band, confirming the histological observations.

### Results of Statistical Analysis

The results of the statistical analysis are given in table 3. Using the combined criteria of PTR and LUM, the highest sensitivities and specificities, 0.81 and 0.87, respectively, were calculated at the D<sub>2</sub> threshold among all the examination methods. In the cases of PTR-only or LUM-only criteria, sensitivities are between 0.52 and 0.69, while specificities are relatively higher, between 0.72 and 0.86. In a manner similar to other researchers' findings [Lussi et al., 2001; Costa et al., 2002; Heinrich-Weltzien et al., 2002; Alwas-Danowska et al., 2002], visual inspection resulted in poor sensitivities (0.51 at D<sub>2</sub> and 0.36 at D<sub>3</sub>) and particularly high specificities (1.00 at both thresholds). Radiographs also exhibited poor sensitivities (0.29 at D<sub>2</sub> and 0.36 at D<sub>3</sub>) and high specificities (1.00 at D<sub>2</sub> and 0.85 at D<sub>3</sub>). The continuous (dc) luminescence method (DIAGNOdent) showed sensitivities of 0.60 at D<sub>2</sub> and 0.76 at D<sub>3</sub>; specificities were 0.78 at D<sub>2</sub> and 0.85 at D<sub>3</sub>. From table 3, it should be noted, however, that a relatively small subset of all our measurement spots was used for obtaining the visual and radiographic statistics, compared to the much more comprehensive sample sizes used for the other methods, especially for PTR and LUM.

## Discussion

Our data indicate that the PTR amplitude and phase curves exhibit curvature when associated with demineralized enamel in the fissure. The frequency where the curvature maximum occurs varies from sample to sample. The frequency dependence of the maximum is believed to be a function of the level or condition of the caries and the depth of the lesion. PTR has been proven to have depth profilometric character: With very low modulation frequencies, we were able to probe deeper layers (up to 5 mm from the surface) [Jeon et al., 2000]. One of the near-future aims of this study will be focused on quantifying the demineralization and identifying healthy fissure geometry effects from carious fissures by exploiting these frequency-domain diffusion-wave characteristics. Thus, PTR amplitude and phase signals may provide detailed information of the deep lesion and/or demineralized zone below the surface of the tooth with their depth profilometric frequency dependence. In summary, table 3 shows that the sensitivity using only PTR or LUM is lower than the specificity. However, by combining PTR and LUM, both amplitudes and phases, the sensitivity is much higher than any other methods used in this study.

In some cases, such as fissure F1 of the tooth in figure 4, histological observation shows apparent demineralized caries into dentin but the PTR and LUM signals have lower amplitude and phase than expected. This is due to the geometrical restriction of our current experimental set-up and can be improved by using a design of the probing tip with an optical fiber to transport visible laser radiation to the tooth, surrounded by coaxially distributed collector fibers to collect synchronous luminescence and IR responses. This configuration, targeted for a modified PTR/LUM set-up in the near future, is expected to allow for a relatively narrow and well-controllable range of solid angles for photon delivery and collection and should largely eliminate geometric artifacts of the surrounding structures.

## Conclusions

Using simultaneous, non-intrusive, non-contacting frequency-domain PTR and LUM imaging techniques, we have been able to detect carious lesions in the occlusal fissures of posterior human teeth. These investigations have been performed with a near-IR source (659-nm wavelength) from a semiconductor

laser. PTR and LUM are able to detect lesions, which are neither visible, nor detectable, with radiographs or with dc luminescence (DIAGNOdent). PTRs operating physical principle of depth-weighted diffuse photon density waves converted to thermal-wave diffusion generate greater sensitivity and contrast to both the presence of, and changes in, sharp boundaries through diffusive confinement, as well as changes in demineralization of the tooth as compared to the uniformly depth-integrated LUM. The sensitivity of depth profilometric PTR to the presence of advanced demineralization within an occlusal fissure and the corroboration of the LUM probe, albeit with diminished depth sensitivity, was demonstrated. More work will be required to sort out signal dependence on the type, size, and severity of sub-surface carious lesions. Thermal-wave confinement within naturally occurring dental layers, such as in the case of variable DEJ depth in the proximal surfaces, can be useful in measuring enamel thickness by means of PTR frequency scans at a fixed spot away from high-curvature surfaces.

In conclusion, the combined wealth of information stemming from 4 PTR and LUM signals (2 amplitudes and 2 phases), including the availability of detailed curve shapes over a wide range of modulation frequencies, was used to examine a large number of spots (280) representing 52 teeth. The study yielded a sensitivity much higher than any of the other methods used in this study, and a specificity comparable to that of dc luminescence diagnostics, although comparisons with DIAGNOdent, radiography, and visual inspection results were made using only a subset of the full set of dental spots examined with PTR/LUM. It is concluded that PTR and LUM has excellent potential to become a sensitive, non-intrusive, depth-profilometric dental probe for the diagnosis of near-surface or deep, sub-surface carious lesions.

### **Acknowledgment**

The support of Materials and Manufacturing Ontario (MMO) with an Enabling Contract is gratefully acknowledged.

### **References**

al-Khateeb S, Exterkate RAM, de Josselin de Jong E, Angmar-Månsson B, ten Cate JM: Light-induced fluorescence studies on dehydration of incipient enamel lesions. *Caries Res* 2002;36:25-30.

Alwas-Danowska HM, Plasschaert AJM, Suliborski S, Verdonschot EH: Reliability and validity issues of laser fluorescence measurements in occlusal caries diagnosis. *J Dentistry* 2002;30:129-134.

Anttonen V, Seppä L, Hausen H: Clinical study of the use of the laser fluorescence device DIAGNOdent for detection of occlusal caries in children. *Caries Res* 2003;37:17-23.

Busse G, Walther HG: Photothermal nondestructive evaluation of materials with thermal waves; in Mandelis A (ed): *Principles & Perspectives of Photothermal & Photoacoustic Phenomena*. Elsevier, New York, 1992; vol 1, pp 205-298.

Clinical Research Associates: Air abrasion caries removal, 5-year status report. *CRA Newsletter* 1999;23:12,2-3.

Costa AM, Yamaguchi PM, De Paula LM, Bezerra ACM: In vitro study of laser diode 655 nm diagnosis of occlusal caries. *J Dent Child* 2002;69:249-253.

Eggertsson H, Analoui M, van der Veen MH, González-Cabezas C, Eckert GJ, Stookey GK: Detection of early interproximal caries in vitro using laser fluorescence, dye-enhanced laser fluorescence and direct visual examination. *Caries Res* 1999;33:227-233.

Heinrich-Weltzien R, Weerheijm KL, Kühnisch J, Oehme T, Stösser L: Clinical evaluation of visual, radiographic, and laser fluorescence methods for detection of occlusal caries. *J Dent Child* 2002;69:127-132.

Hibst R, Gall R, Klafke M: Device for the recognition of caries, plaque or bacterial infection on teeth. *US Pat* 2000; 6,024,562.

Hibst R, Paulus R: Caries detection by red excited fluorescence: Investigations on fluorophores. *Caries Res* 1999;33:295.

Hibst R, König K: Device for detecting dental caries. *US Pat* 1994; 5,306,144.

Jeon RJ, Mandelis A, Sanchez V, Abrams SH: Non-intrusive, non-contacting frequency-domain photothermal radiometry and luminescence depth profilometry of carious and artificial sub-surface lesions in human teeth. *J Biomed Opt* 2003 (submitted).

Lagerweij MD, van der Veen MH, Ando M, Lukantsova L, Stookey GK: The validity and repeatability of three light-induced fluorescence systems: An in vitro study. *Caries Res* 1999;33:220-226.

Lussi A, Imwinkelried S, Pitts NB, Longbottom C, Reich E: Performance and Reproducibility of a Laser Fluorescence System for Detection of Occlusal Caries in vitro. *Caries Res* 1999;33:261-266.

Lussi A, Megert B, Longbottom C, Reigh E, Francescut P: Clinical performance of a laser fluorescence device for detection of occlusal caries lesions. *Eur J Oral Sci* 2001;109:14-19.

Mandelis A: Review of progress in theoretical, experimental, and computational investigations in turbid tissue phantoms and human teeth using laser infrared photothermal radiometry; in Maldague XP and Rozlosnik AE (ed): *Thermosense XXIV, Proc SPIE*, 2002, vol 4710, pp 373-383.

Mandelis A, Munidasa M, Othonos A: Single-ended infrared photothermal radiometric measurement of quantum efficiency and metastable lifetime in solid-state laser materials: The case of ruby ( $\text{Cr}^{3+}:\text{Al}_2\text{O}_3$ ). *IEEE J Quant Electron* 1993;29:1498-1504.

## DENTAL DEPTH PROFILOMETRIC DIAGNOSIS OF PIT & FISSURE CARIES

Mandelis A, Nicolaidis L, Feng C, Abrams SH: Novel dental depth profilometric imaging using simultaneous frequency-domain infrared photothermal radiometry and laser luminescence; in Oraevsky A (ed): Biomedical Optoacoustics. Proc SPIE, 2000; vol 3916, pp 130-137.

McComb D, Tam LE: Diagnosis of occlusal caries: Part I. Conventional methods. J Can Dent Assoc 2001;67:454-457

Munidas A, Mandelis A: Photothermal imaging and microscopy; in Mandelis A (ed): Principles & Perspectives of Photothermal & Photoacoustic Phenomena. Elsevier, New York, 1992; vol 1, pp 299-367.

Nicolaidis L, Feng C, Mandelis A, Abrams SH: Quantitative dental measurements by use of simultaneous frequency-domain laser infrared photothermal radiometry and luminescence. Appl Opt 2002;41:768-777.

Nicolaidis L, Mandelis A, Abrams SH: Novel dental dynamic depth profilometric imaging using simultaneous frequency-domain infrared photothermal radiometry and laser luminescence. J Biomed Opt 2000;5:31-39.

Ricketts D, Kidd E, Weerheijm K, de Soet H: Hidden caries: What is it? Does it exist? Does it matter? Int Dent J 1997;47:259-265.

Shi XQ, Tranæus S, Angmar-Månsson B: Comparison of QLF and DIAGNOdent for Quantification of Smooth Surface Caries. Caries Res 2001;35:21-26.

Shi XQ, Welander U, Angmar-Månsson B: Occlusal caries detection with KaVo DIAGNOdent and radiography: An in vitro comparison. Caries Res 2000;34:151-158.

Welsh GA, Hall AF, Hannah AJ, Foye RH: Variation in DIAGNOdent measurements of stained artificial caries lesions. Caries Res 2000;34:324.